University of Groningen

Zoledronate Derivatives as Potential Inhibitors of Uridine Diphosphate-Galactose Ceramide Galactosyltransferase 8

Pannuzzo, Giovanna; Graziano, Adriana Carol Eleonora; Pannuzzo, Martina; Masman, Marcelo Fabricio; Avola, Rosanna; Cardile, Venera

Published in:
Journal of Neuroscience Research

DOI:
10.1002/jnr.23761

IMPORTANT NOTE: You are advised to consult the publisher's version (publisher's PDF) if you wish to cite from it. Please check the document version below.

Document Version
Publisher's PDF, also known as Version of record

Publication date:
2016

Link to publication in University of Groningen/UMCG research database

Citation for published version (APA):
Pannuzzo, G., Graziano, A. C. E., Pannuzzo, M., Masman, M. F., Avola, R., & Cardile, V. (2016). Zoledronate Derivatives as Potential Inhibitors of Uridine Diphosphate-Galactose Ceramide Galactosyltransferase 8: A Combined Molecular Docking and Dynamic Study. *Journal of Neuroscience Research*, *94*(11), 1318-1326. https://doi.org/10.1002/jnr.23761

Copyright
Other than for strictly personal use, it is not permitted to download or to forward/distribute the text or part of it without the consent of the author(s) and/or copyright holder(s), unless the work is under an open content license (like Creative Commons).

The publication may also be distributed here under the terms of Article 25fa of the Dutch Copyright Act, indicated by the "Taverne" license. More information can be found on the University of Groningen website: https://www.rug.nl/library/open-access/self-archiving-pure/taverne-amendment.

Take-down policy
If you believe that this document breaches copyright please contact us providing details, and we will remove access to the work immediately and investigate your claim.

Downloaded from the University of Groningen/UMCG research database (Pure): http://www.rug.nl/research/portal. For technical reasons the number of authors shown on this cover page is limited to 10 maximum.

Journal of Neuroscience Research 94:1318–1326 (2016)

Zoledronate Derivatives as Potential Inhibitors of Uridine Diphosphate-Galactose Ceramide Galactosyltransferase 8: A Combined Molecular Docking and Dynamic Study

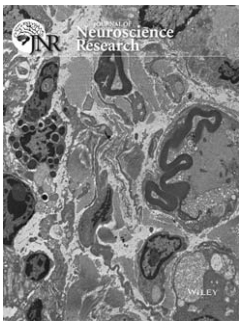

Giovanna Pannuzzo,[1] Adriana Carol Eleonora Graziano,[1] Martina Pannuzzo,[2] Marcelo Fabricio Masman,[3] Rosanna Avola,[1] and Venera Cardile[1]*

[1]Department of Biomedical and Biotechnological Sciences, Section of Physiology, University of Catania, Catania, Italy
[2]Department of Computational Biology, Universität Erlangen-Nürnberg, Erlangen, Germany
[3]Department of Biocatalysis and Biotransformation, Groningen Biomolecular Sciences and Biotechnology Institute, University of Groningen, Groningen, The Netherlands

Krabbe's disease is a neurodegenerative disorder caused by deficiency of galactocerebrosidase activity that affects the myelin sheath of the nervous system, involving dysfunctional metabolism of sphingolipids. It has no cure. Because substrate inhibition therapy has been shown to be effective in some human lysosomal storage diseases, we hypothesize that a substrate inhibition therapeutic approach might be appropriate to allow correction of the imbalance between formation and breakdown of glycosphingolipids and to prevent pathological storage of psychosine. The enzyme responsible for the biosynthesis of galactosylceramide and psychosine is uridine diphosphate-galactose ceramide galactosyltransferase (2-hydroxyacylsphingosine 1-β-galactosyltransferase; UGT8; EC 2.4.1.45), which catalyzes the transferring of galactose from uridine diphosphate-galactose to ceramide or sphingosine, an important step of the biosynthesis of galactosphingolipids. Because some bisphosphonates have been identified as selective galactosyltransferase inhibitors, we verify the binding affinity to a generated model of the enzyme UGT8 and investigate the molecular mechanisms of UGT8–ligand interactions of the bisphosphonate zoledronate by a multistep framework combining homology modeling, molecular docking, and molecular dynamics simulations. From structural information on UGTs' active site stereochemistry, charge density, and access through the hydrophobic environment, the molecular docking procedure allowed us to identify zoledronate as a potential inhibitor of human ceramide galactosyltransferase. More importantly, zoledronate derivates were designed through computational modeling as putative new inhibitors. Experiments in vivo and in vitro have been planned to verify the possibility of using zoledronate and/or the newly identified inhibitors of UGT8 for a substrate inhibition therapy useful for treatment of Krabbe's disease and/or other lysosomal disorders. © 2016 Wiley Periodicals, Inc.

Key words: Krabbe disease; ceramide galactosyltransferase; substrate deprivation therapy; molecular docking; molecular dynamics; homology modeling

Krabbe's disease is classified as a lysosomal storage disorder (LSD). In the treatment of some LSDs, substrate deprivation therapy (or substrate reduction therapy) has been shown to be effective (Platt and Jeyakumar, 2008). In fact, clinical studies on patients suffering from LSDs, such as Niemann-Pick C and Sanfilippo, have demonstrated that substrate deprivation therapy might be effective in humans, not only in delaying the appearance of

SIGNIFICANCE

In this study, by a combined computational approach, zoledronate emerged as an optimal inhibitor of human ceramide galactosyltransferase. Moreover, using the AutoGrow algorithm, we designed several new zoledronate derivatives. Our information is useful as a first step toward a possible substrate inhibition therapy to be suggested to Krabbe's disease patients.

G. Pannuzzo and A.C.E. Graziano contributed equally to this work.

Contract grant sponsor: Progetto Grazia, Associazione Italiana per la Leucodistrofia di Krabbe; Contract grant number: 15048720

*Correspondence to: Venera Cardile, PhD, Department of Biomedical and Biotechnological Sciences, Section of Physiology, University of Catania, Via S. Sofia 64, 95125 Catania, Italy. E-mail: cardile@unict.it

Received 28 January 2016; Revised 29 March 2016; Accepted 14 April 2016

Published online 17 September 2016 in Wiley Online Library (wileyonlinelibrary.com). DOI: 10.1002/jnr.23761

© 2016 Wiley Periodicals, Inc.

symptoms or halting the progress of the disease but also in reversing some of the neurological symptoms (Patterson et al., 2007; Piotrowska et al., 2008).

In Krabbe's disease, the enzyme galactosylceramidase does not work properly; galactosylceramide and psychosine cannot be degraded as usual, and the accumulation of psychosine in the brain leads to apoptosis of oligodendrocytes, progressive demyelination, and the appearance of large, multinuclear cells (globoid cells) derived from microglia (Tanaka et al., 1993).

The enzyme responsible for the biosynthesis of galactosylceramide and psychosine is uridine diphosphate (UDP)-galactose ceramide galactosyltransferase (UGT8). The UGT8 family contains only one member, UGT8A1, that has a biosynthetic role in the nervous system (Mackenzie et al., 2005). To allow the correction of the imbalance between formation and breakdown of galactosylceramide and psychosine, a reduced biosynthesis of glycosphingolipids has been proposed by the inhibition of UGT8 (Pannuzzo et al., 2010). This enzyme has been suggested to play a critical role in myelin formation (Costantino-Ceccarini and Suzuki, 1975), signal transduction (Dyer and Benjamins, 1991; Joshi and Mishra, 1992), viral and microbial adhesion (Khan et al., 1996), and oligodendrocyte development (Mirsky et al., 1980).

The substrate reduction therapeutic approach has been validated with galactosylceramide synthase inhibitors. However, the efficacy of these compounds is limited because of low central nervous system (CNS) penetration, limited ability to reduce galactosphingolipid synthesis through the inhibition of upstream precursors (galactosylceramide), and dose-limiting toxicity (Bansal, 1989; Butters et al., 2005). A more recent class of galactosyltransferase inhibitors comprises N-alkylated derivatives of deoxynojirimycin and deoxygalactonojirimycin and derivatives of methylene diphosphonate or bisphosphonates such as sodium alendronate, sodium etidronate, zoledronate, and others (Takayama et al., 1999).

Bisphosphonates are used in the treatment of patients with osteoporosis and malignant osteolytic diseases, hypercalcemia of malignancy, multiple myeloma, postmenopausal osteoporosis, and tumor-associated osteolysis (Zara et al., 2015). They are small-molecular-size (less than 300 Da) organic pyrophosphate analogs in which two phosphates are connected by a carbon atom (P–C–P) with various side chains. This chemical structure gives them resistance to enzymatic degradation (Lezcano et al., 2014). They have the advantage of mimicking the transition state of the nucleotide portion of UDP-galactose (UDP-gal), a natural substrate of UGT8. Moreover, they are easy to synthetize and derivatize, are physiologically stable, and have low toxicity (Takayama et al., 1999; Brown and Zacharin, 2009; Barros et al., 2012). Only one case, a 7-year-old child who developed clinical features of a severe systemic inflammatory response following zoledronic acid infusion, has recently been reported (Trivedi et al., 2016). However, these authors recognized the complexity of the child's underlying medical conditions. He had previously been treated with four cycles of pamidronate, and his home medications included but were not limited to bactofen, clonazepam, gabapentin, levetiracetam, levocarnitine, levothyroxine, and calcium carbonate, a complex medical history (Trivedi et al., 2016).

Therefore, the current study performs a molecular docking to predict the binding affinity of the bisphosphonate zoledronate with a generated model of UGT8 to highlight a potential inhibitive activity. The homology model is required because of the lack of crystallographic or nuclear magnetic resonance (NMR) data on UGT8. Among the various bisphosphonates, we use bisphosphonate zoledronate because it possesses the potential to form hydrogen bonds and has low steric hindrance that could favor an optimal fit into the probable site of binding.

To confirm docking results and for understanding more deeply at the atomic level, we carry out molecular dynamics simulations. Furthermore, using the AutoGrow algorithm, we design several new putative inhibitors with stronger affinity for UGT8 compared with zoledronate.

MATERIALS AND METHODS

Homology Modeling

The first step of homology modeling is to recognize the template that we made in BLAST (basic local alignment search tool; htpp://www.ncbi.nlm.nih.gov/blast/; Wong et al., 2011). To increase the precision of the comparative model created, we used the program YASARA (yet another scientific artificial reality application; http://www.yasara.org/), a self-parameterizing force field. For the purpose of generating a homology model of UGT8, the sequence of 541 amino acids of the human 2-hydroxyacylsphingosine 1-β-galactosyltransferase isoform X1 (NCBI reference sequence XP_006714365.1), the YASARA's fully automated module homology modeling (CASP protocol) generator for this task (Krieger et al., 2009), and the homology modeling parameters were used. Slow protocol included three PSI-BLAST iterations in template search; maximum allowed (PSI)-BLAST E-value to consider template (EValue Max) was set to 0.5; 10 templates were allowed; the maximum number of templates with the same sequence was set to 5; the maximum oligomerization state was set to 4; a maximum of 10 alignments variations per template; 100 conformations were tried per loop generation; and a maximum of 10 residues was allowed to be added to the termini (Altschul et al., 1990, 1997).

Target Protein Acquisition

Protein templates, UDP-gal, and zoledronate were downloaded from the online protein data bank (PDB; http://www.rcsb.org/pdb; Schäffer et al., 2001). The structure of the ligand uridine diphosphate galactose was downloaded from the complex with β-1.4 galactosyltransferase (PDB: 1TW1) and the structure of zoledronate from the complex with farnesyl diphosphate synthase (PDB: 2F8C). In both cases, the protein was subsequently removed, and the structures were subjected to energy minimization in an environment that mimics the low dielectric conditions of the organic solvent (vacuum).

TABLE I. Summary of the 10 Best Templates Used for Generation of the UGT8 Model*

Template	Total score	BLAST E-value	Align score	Identity (%)	PDB ID	Resolution (Å)
1	85.48	5e-82	438.0	47	2O6L	1.80
2	56.75	2e-21	136.0	30	3HBF	2.10
3	51.21	2e-21	136.0	30	3HBJ	2.10
4	50.55	3e-24	115.0	27	2PQ6	2.10
5	36.13	8e-18	78.0	25	2VCE	1.90
6	33.65	3e-21	78.0	25	2C1X	1.90
7	33.59	3e-21	78.0	25	2C1Z	1.90
8	32.58	7e-20	70.0	23	2ACV	2.00
9	32.25	3e-21	78.0	25	2C9Z	2.10
10	29.72	8e-16	67.0	26	3IA7	1.91

*Total score and align score values correspond to the YASARA z-score range; Identity corresponds to the percentile of sequence identity of the given template and the target sequence UGT8.

The energies of the protein, the ligand, and the inhibitors were minimized by steepest descent algorithm. Simulations were performed in GROMACS (Groningen machine for chemical simulations; http://www.gromacs.org/) version 4.5.4 simulation package, and GROMOS (Groningen molecular simulation) 53A6 force field was used to describe atomistically receptor, ligands, and inhibitors (Hess et al., 2008).

Generation of Putative Inhibitors: Zoledronate Derivatives

To generate putative inhibitors based on zoledronate, we used the AutoGrow 3.0 (http://autogrow.ucsd.edu/; Durrant et al., 2013) algorithm that can either generate novel predicted inhibitors ex nihilo from very basic starting structures or optimize existing inhibitors to improve the binding affinity. We chose the second approach. We allowed five generations of productions based in a starting pool of 20 compounds (including zoledronate). A medium-sized library of fragments (~150 g/mol) was used for new inhibitor production. Five mutants and five crossovers were allowed for each generation. AutoDock Vina (http://vina.scripps.edu/) was used for this purpose (Trott and Olson, 2010).

Molecular Docking

Docking calculations were carried out in AutoDock 4.0. It is one of the most suitable programs for performing molecular docking of ligands to their macromolecular receptors and discriminating potential inhibitors. The human ceramide galactosyltransferase was docked with UDP-gal, zoledronate, and the putative inhibitors a–g (chemical structures reported in Table II). The free energy of binding (ΔG) of docked complexes was then generated in this molecular docking software with the Lamarckian genetic algorithm to search for the best conformers (Bikadi and Hazai, 2009).

The graphical user interface program AutoDock tools was used to prepare, run, and analyze the docking simulations. The grid points and spacing were computed in AutoGrid (Redwood Shores, CA; (Morris et al., 1998). The grid must surround the region of interest into the macromolecule. The spacing between grid points was 0.37 Å for active site and 1 Å for blind docking. During the docking process, a maximum of 100 conformers was considered for each compound. The population size was set to 150, and the individuals were randomly initialized.

For UGT8 preparation, polar hydrogens were added, and then Kollman united atom charges and atomic solvation parameters were assigned. For ligand preparation, Gasteiger partial charges were added, nonpolar hydrogen atoms were merged, and rotatable bonds were defined.

A preliminary blind docking study was performed to discriminate the preferential binding sites of the ligand to the receptor. To this end, for the first simulation, the grid size was properly set up to contain the entire receptor structure (40, 40, 40 Å along x, y, z, respectively, space between grid points of 1 Å). Next, we selected the pose of the ligand into the active site, and the grid was centered on this catalytic active region of the receptor (50, 50, 50 points along x, y, z, respectively, space between grid points of 0.37 Å).

Molecular Dynamics

The UGT8 binding domain was complexed with the several selected inhibitors from the previous docking study and then embedded in a water box in the presence of salt (Na^+Cl^-) and simulated for 20 nsec. The solution was electroneutral. We chose as a reference structure for ligands the configuration with higher level of affinity for the enzymatic active site. Periodic boundary conditions were applied to the three dimensions of the box.

Simulations were performed in the GROMACS version 4.5.4 simulation package (Hess et al., 2008), and the GROMOS 53A6 force field was used for protein and ligands (Oostenbrink et al., 2005). The Berendsen weak coupling temperature and pressure coupling algorithms (Berendsen et al., 1984) were used with coupling constants of 0.3 psec and 3.0 psec, respectively. Protein, ligand, and water ions were separately coupled to a heat bath. The Lennard-Jones potential was smoothly shifted to zero between 9 and 12 Å. For electrostatics, we used the particle mesh Ewald scheme.

Each system was minimized by the steepest descent algorithm after the molecular species had been added and then equilibrated in NpT ensemble for 10 psec prior to data collection. After this time, ligands were stably bound to the protein domain. The time step was set to 0.002 psec.

TABLE II. Docking Results of UDP-gal, Zoledronate, and Inhibitors a–g in Complex With UGT8

Compound	Binding energy (ΔG; (kcal/mol)	No. of hydrogen bonds	Amino acid acceptors of hydrogen bonds	Interacting residues
UDP-gal 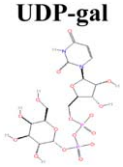	–7.5	6	A295, G296, R322, Q343, N362, S363	A295, G296, R322, Q343, H358, N362, S363, F380, H383
Zoledronate 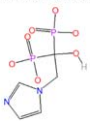	–5.7	4	A295, R322, Q343, S363	G294, A295, R322, Q343, H358, G360, L361, N362, S363, H383
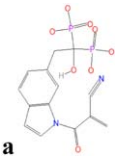 **a**	–6.9	5	R322, Q343, H358, N362 S363	G294, A295, R322, Q343, H358, L361, N362, S363, F380, D382, H383
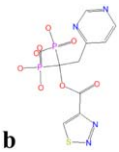 **b**	–6.2	5	A295, R322, H358, N362, S363	G294, A295, R322, Q343, H358, G360, N362, S363, H383
c	–6.0	5	R322, Q343, H358, N362, S363	A295, G296, R322, Q343, H358, G360, N362, S363, F380
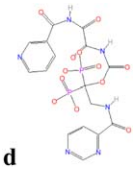 **d**	–6.1	4	A295, L341, S363(HN1), S363(HG1)	A295, R322, W340, L341, Q343, H358, G360, N362, S363
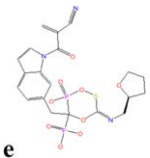 **e**	–7.5	5	A295, R322, Q343, N362, S363	A295, R322, Q343, L361, N362, S363, F380
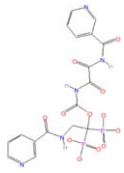 **f**	–6.2	3	R322, N344, N362	G294, R322, W340, P342, Q343, N344, D345, H358, N362, S363
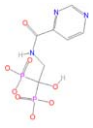 **g**	–6.2	5	A295, R322, Q343, N362, S363	G294, A295, R322, Q343, H358, N362, S363, F380, H383

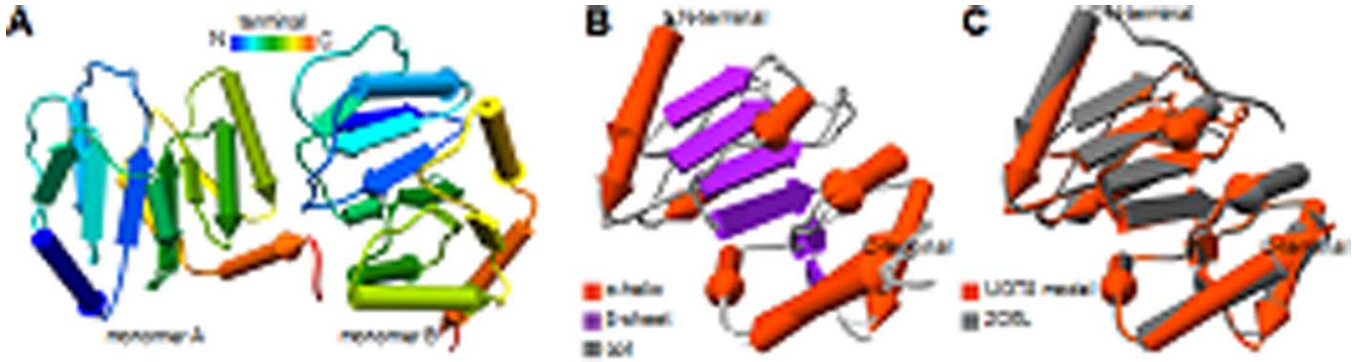

Fig. 1. 3D representation of the homology model created for UGT8. **A**: The homodimeric model, in which residues are color-coded according to their position in the sequence (color gradient from blue (N-terminal) to red (C-terminal). **B**: The superimposed monomers (chains A and B), in which residues are color coded by secondary structure composition (orange, α-helix; purple, β-sheet; gray, coil). 2O6L was found to be the best template candidate for the creation of this homology model. **C**: Superimposed structures of the model of UGT8 (orange) and crystal structure of 2O6L.

RESULTS

Homology Modeling

The homology model created for UGT8 was based on the structural information of 10 crystal structures that served as structural templates. Table I summarizes the templates selected for this purpose. Although the complete sequence of UGT8 (451 residues) was subjected to homology modeling generation, only the C-terminal (residues 267–435) fraction possessed enough structural information to yield a homology model. The UDP-glucuronosyltransferase 2B7 (PDB: 2O6L) was shown to be the best structural match for UGT8 model creation, with a sequence identity of 47% (Kopp and Schwede, 2004).

The YASARA (Krieger et al., 2002) protocol created a hybrid model resulting from the combination of the best parts of the 56 models, hoping to increase the accuracy beyond each of the contributors. The main contributor to the hybrid model was the best scoring model created on the structural template 2O6L and several other different fragments successfully copied from other models. Because the hybrid model scored better than all previous models, it was saved as the final model and used for further docking and molecular dynamic simulations. Figure 1 shows the hybrid model of UGT8 in homodimeric state (Fig. 1A), overlapped monomers A and B (Fig. 1B), and the superposition of monomer A with the 2O6L crystal structure (Fig. 1C).

Molecular Docking

UDP-gal, the known natural substrate for UGT8, was the first compound analyzed. The best conformations had binding energies in the ranges of –7.6 and –6.5 kcal/mol. Two different binding loops of the protein were identified, one of which, showing affinity of –7.5 kcal/mol, corresponded to the binding site already described for other UGT enzymes (Li and Wu, 2007; Locuson and Tracy, 2007; Miley et al., 2007). In looking in detail at the interactions between this conformer and the binding site, the following amino acids were involved: A295, G296, R322, Q343, H358, N362, S363, F380, H383 (Fig. 2).

The predicted interacting residues were divided into three different groups of residues interacting with 1) nucleotide, 2) phosphate, or 3) UDP-gal. From previous studies on other UGT enzymes, in particular, UGT1A6 and UGT3A1, amino acids Q343 (corresponding to Q356 in UGT1A6 and Q354 in UGT3A1), E366 (corresponding to E379 in UGT1A6 and E377 in UGT3A1), and R322 (corresponding to R335 in UGT1A6 and R333 in UGT3A1) were predicted to make contact with the uracil base. Amino acids S363 (S376 in UGT1A6 and S374 in UGT3A1) and N362 (corresponding to N375 in UGT1A6 and N373 in UGT3A1) were predicted to form hydrogen bonds with the oxygen of the diphosphate; H358 (corresponding to H371 in UGT1A6 and H369 in UGT3A1) was predicted to interact with sugar (Offen et al., 2006; Li and Wu, 2007; Locuson and Tracy, 2007). The main carbonyl chain was predicted to interact with –NH of L341 (corresponding to L354 in UGT1A6 and L352 in UGT3A1; Shao et al., 2005). These interactions have been found in several other GT-B enzyme structures (Bolam et al., 2007; Li and Wu, 2007; Locuson and Tracy, 2007).

Zoledronate was the second compound analyzed. The best conformations had binding energies ranging from –5.7 to –5.1 kcal/mol, and two preferential binding loops of the protein were identified; the preferential conformation corresponds to the hypothesized binding site. In looking in detail at the interactions between the best conformer and the binding site, the following amino acids appear to be directly involved: GLY 294 (G294), ALA 295 (A295), ARG 322 (R322), GLN 343 (Q343), HIS 358 (H358), GLY 360 (G360), LEU 361 (L361), ASN 362 (N362), SER 363 (S363), HIS 383 (H383; Fig. 2).

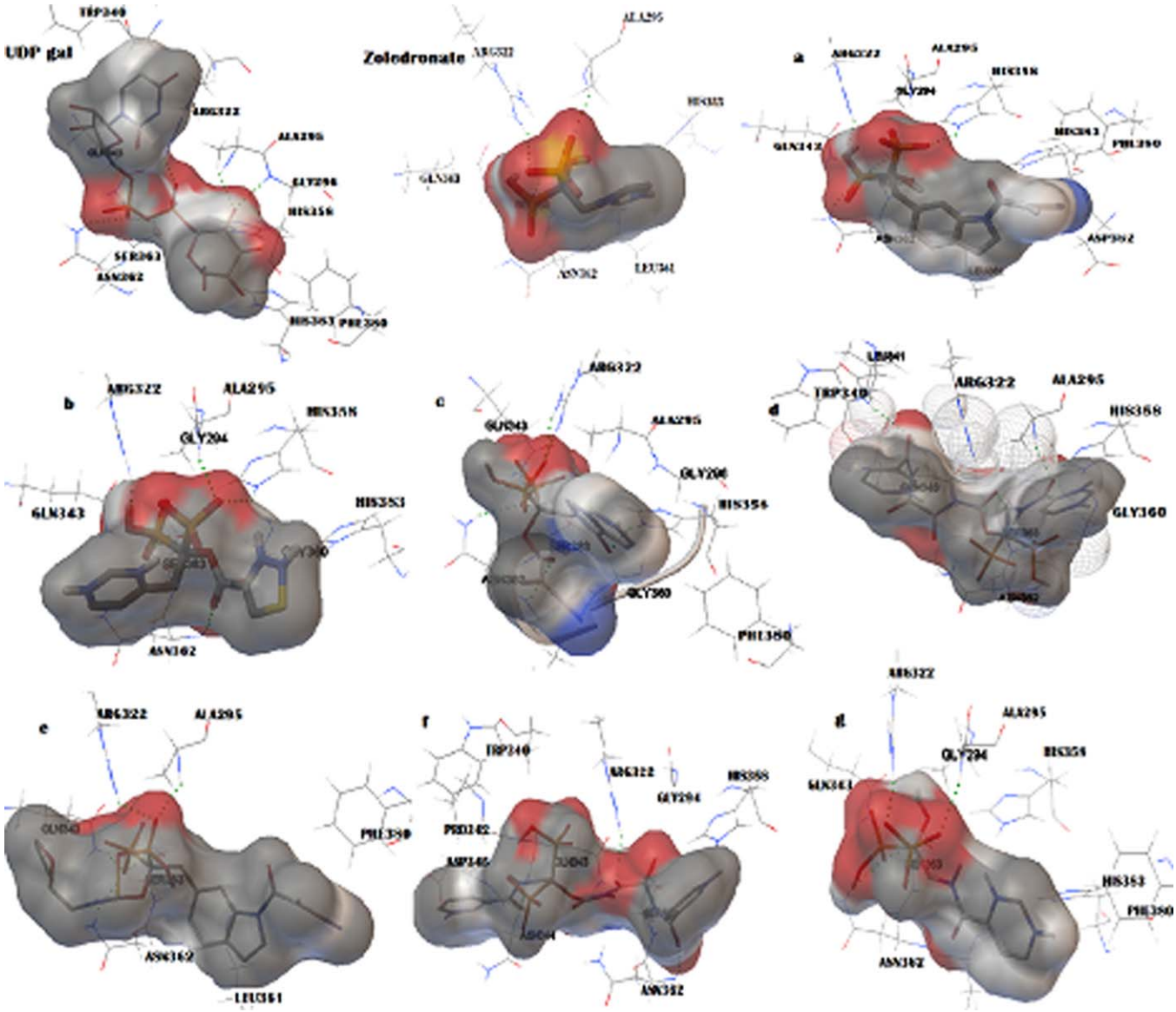

Fig. 2. 3D interaction map showing the catalytic amino acids for interaction with UGT8 of UDP-gal; zoledronate; and the compounds a–g.

The results of molecular docking for the other inhibitors (a–g) are displayed in Table II, and the specific interactions between the several ligands and the receptor are displayed in Figure 2. These designed putative inhibitors (a–g) were electronegative, demonstrating good UGT8 hydrogen-bond attractions; their binding energy was greater compared with zoledronate and more similar to UDP gal.

Dynamic Complexes

To shed some light on a more realistic approach to these interactive systems and acknowledging the limitations of the docking approach, we carried out some molecular dynamics (MD) simulations to observe their dynamics properties. In all the investigated systems, the ligand stably bound the enzyme domain over 20 nsec of simulation (Fig. 3a). Most of them (b–g and zoledronate) spent time in a specific region where the same residues previously identified by the docking study and suggested experimentally were protruding, supporting once again the results reported (Fig. 3b). Zoledronate, in particular, showed the capability to penetrate deeper into the pocket size, probably because of the smaller steric hindrance, allowing a tighter contact with the enzyme.

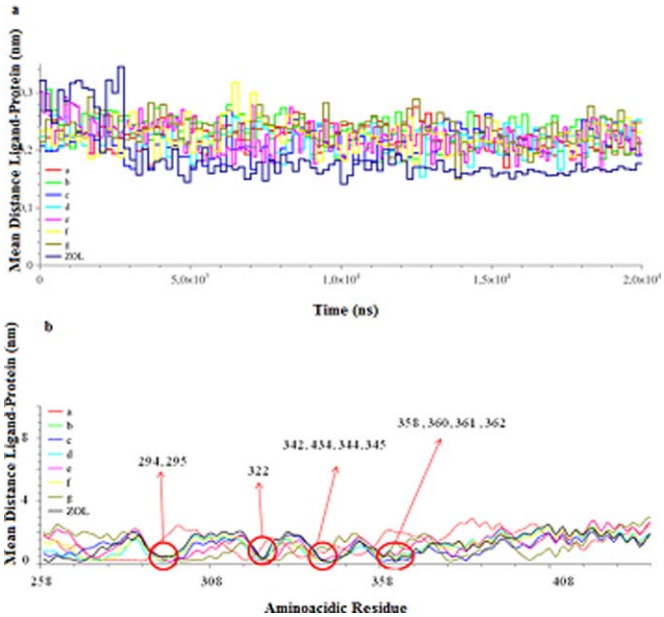

Fig. 3. **a**: Protein–ligand mean distance profiles over 20 nsec of simulation. **b**: Contact profiles of the ligands with the protein residues. Binding energies (coulombic and Lennard-Jones interactions) in all cases assume negative values, indicative of a favorite and stable binding.

DISCUSSION

Krabbe's disease has no cure, although various treatments have been attempted on humans and in animal models, with varying degrees of success. Among these, substrate reduction therapy seeks to inhibit the rate of synthesis of glycosphingolipids to levels at which the residual activity of the mutant catabolic enzyme is sufficient to prevent pathological storage (Butters et al., 2005). L-cycloserine is an irreversible inhibitor of 3-ketodihydrosphingosine synthetase, which is the first enzyme of the sphingolipid pathway. Substrate reduction therapy with L-cycloserine has been evaluated in the murine model of Krabbe's disease for over 15 years and has been shown to improve the life span of the twitcher mouse significantly when given alone (LeVine et al., 2000), synergizing with bone marrow therapy (Biswas and Levine, 2002) and CNS-directed gene therapy (Hawkins-Salsbury et al., 2015) to extend life span. However, L-cycloserine inhibits the synthesis of numerous glucosylated and galactosylated lipids, resulting in untoward nonspecific effects and greatly limiting the translational potential of this therapy beyond the murine model. Therefore, investigation of alternative substrate reduction targets is warranted. In this research, a molecular docking and dynamics simulations study was performed to evaluate the capability of zoledronate and seven additional compounds generated in silico to inhibit the enzyme UGT8. Our goal was to find a new compound to suggest as a potential substrate reduction therapy for Krabbe's disease.

It is known that the accurate prediction of the binding modes between the ligand and protein is of fundamental importance in modern structure-based drug design. In this research, the lack of data for glycosyltransferases made it difficult to design structure-based inhibitors. In addition, the transition state of the enzymatic reaction requires the presence of the nucleotide, metals, acceptor sugar, and donor sugar, all of which are complex components to mimic. Furthermore, for molecular docking, three-dimensional (3D) structure of the macromolecule UGT8 is required; unfortunately, for our study, neither crystallographic nor NMR data were available. To overcome this limitation, we used combined homology modeling with molecular docking to build a 3D model of the enzymatic active site. The deduced amino acid sequence of human UGT8 revealed that a 61-kDa protein of 541 amino acid residues, 21 of which are charged and encoded by a gene of five exons on chromosome 4q26 UGT8, had a high degree of sequence similarity with glucuronosyltransferases (UGT; Schulte and Stoffel, 1993; Stahl et al., 1994). Recently, sequence identity analysis allowed identification of some crystallized glucuronosyltransferases as homologues of UGT8 and prediction of its secondary structure (Krieger et al., 2002, 2009). It is important to point out that the homology model on which our experiments are founded is based on only 168 residues of the C-terminal of UGT8. Furthermore, the sequence identity of the model is <50%. This might seem to limit our model, but it is in line with what has been reported in most studies in which homologous protein models have been designed (Vyas et al., 2012). Moreover, compared with UDP-gal (–7.6 and –6.5 kcal/mol) and other generated compounds, the binding energy of zoledronate was lower. However, the binding energy should be considered together with other important interactions, such as intermolecular, H-bond, and hydrophobic interactions, which can be used to rank the poses from the number of favorable interactions counted. In general, the docking programs miss one important term in binding the energy of ligand to receptor, which is the term *entropic*. This term can be decomposed in rotational, translational, vibrational, and conformational entropies, in which the first two and the last one may be significant. The major information from docking software poses is binding modes, that is, the relative orientation of ligands and w.r.t. protein and their conformations.

Furthermore, we are aware that the quality of the docking simulations can depend significantly on how the input is prepared and how the software parameters are set. Docking does not necessarily provide an accurate assessment of how well the software will perform when screening for new ligands (Sun et al., 2013), so assessing the ability of the docking program to model or accommodate conformational change in the protein, at least at the side-chain level, is crucial. Moreover, the quality of sampling the correct binding mode for a ligand vs. identifying that binding mode by correctly scoring or ranking should be taken into account for a wider understanding of the studied systems. Although it is known that the binding

affinities predicted by docking simulation are not fully trustable, we used them as a general, comparative guide.

In general, the force fields that govern the binding energies are not entirely reliable in docking programs that use them as part of the scoring function. Many researchers place more value on the resulting poses over the binding energy values. There are several articles showing that a docking→MD→MM(GB/PB)SA workflow yields favorable results in terms of ranking ligands. In fact, our approach was in the direction Docking→MD→AutoGrow. For a more quantitative way of comparing the stability of complex with experimental results, poses taken from docking software were further studied with MD simulations to compute the binding energies with all, including entropic, terms.

Experimentally speaking, binding energies are good metrics for ranking ligands that target a specific pocket. However, because of the approximations made in theoretical modeling, one has to assess the theory level that is used in predicting the binding energies. Rigid docking by itself has many assumptions built into it with respect to the idea of modeling a ligand bound to a pocket, including the use of (in general) a solid-phase protein structure, the lack of ligand and binding site conformational dynamics, choice of scoring function, how water is modeled, and others. Nevertheless, many researchers have had success using docking for identifying lead compounds.

In the current study, from homology modeling, the 3D structure of UDP-glucuronosyltransferase 2B7 was validated and selected for use in simulation. Molecular docking allowed us to make a preliminary analysis of the interactions between substrate and enzyme after defining the binding site. The combined use of docking and MD simulations helped us to investigate better these interactions and the binding affinity between UGT8 with UDP-gal and the inhibitor zoledronate as well as providing useful information for the design of other potential drugs. The identified residues of the pocket enzyme interacting with UDP-gal were quite consistent with previous modeling studies (Offen et al., 2006; Li and Wu; 2007). MD simulations were performed in GROMACS, a molecular dynamics package designed primarily for simulations of proteins, lipids, and nucleic acids. GROMACS supports several implicit solvent models as well as new free-energy algorithms, and the software uses multithreading for efficient parallelization even on low-end systems, including Windows-based workstations.

From our combined computational approach, zoledronate emerged as an optimal inhibitor of human ceramide galactosyltransferase. This specific ligand is characterized by a favorable steric hindrance factor in contrast to other inhibitors or UDP-gal. Moreover, it exhibits binding sites distributed homogeneously that can bind simultaneously, giving reason to a perfect match with the enzymatic active site. For these reasons, we believe that zoledronate could represent an efficient candidate for substrate deprivation therapy in Krabbe's disease and other LSDs.

Finally, AutoGrow allowed us to design new potential inhibitors of UGT8. AutoGrow is a new computer-aided drug design algorithm that uses a growing strategy to build upon an initial "core" scaffold. Molecular fragments are added at random to this scaffold, thereby generating a population of novel ligands. These ligands are subsequently docked into the target protein receptor. An evolutionary algorithm evaluates the docking scores of each population member, and the best binders become founders of the subsequent generation. As generation after generation is created, each based on the fit individuals of the previous generation, a larger inhibitor with greater predicted binding affinity eventually evolves. Of course, experiments in vivo and in vitro have been planned to verify the value of using zoledronate and/or the newly identified inhibitors of UGT8 for a substrate inhibition therapeutic approach for treatment of Krabbe's disease and other lysosomal disorders.

CONFLICT OF INTEREST STATEMENT

All authors have no known or potential conflicts of interest.

ROLE OF AUTHORS

All authors had full access to all the data in the study and take responsibility for the integrity of the data and the accuracy of the data analysis. Study concept and design: GP, MP, ACEG. Acquisition of data: MFM, RA. Analysis and interpretation of data: MFM. Drafting of the article: VC. Study supervision: VC. Obtained funding: VC.

REFERENCES

Altschul SF, Gish W, Miller W, Myers EW, Lipman DJ. 1990. Basic local alignment search tool. J Mol Biol 215:403–410.

Altschul SF, Madden TL, Schäffer AA, Zhang Z, Miller W, Lipman DJ. 1997. Gapped BLAST and PSI-BLAST: a new generation of protein database search programs. Nucleic Acid Res 25:3389–3402.

Bansal R, Pfeiffer SE. 1989. Reversible inhibition of oligodendrocyte progenitor differentiation by a monoclonal antibody against surface galactolipids. Proc Natl Acad Sci U S A 86:6181–6185.

Barros ER, Saraiva GL, de Oliveira TP, Lazaretti-Castro M. 2012. Safety and efficacy of a 1-layer treatment with zoledronic acid compared with pamidronate in children with osteogenesis imperfecta. J Pediatr Endocr Metab 25:485–491.

Berendsen HJC, Postma JPM, van Gunsteren WF, Di Nola A, Haak JR. 1984. Molecular dynamics with coupling to an external bath. J Chem Phys 81:3684.

Bikadi K, Hazai Z. 2009. Application of the PM6 semiempirical method to modeling proteins enhances docking accuracy of AutoDock. J Cheminform 11:1–15.

Biswas S, LeVine SM. 2002. Substrate-reduction therapy enhances the benefits of bone marrow transplantation in young mice with globoid cell leukodystrophy. Pediatr Res 51:40–47.

Bolam DN, Roberts S, Proctor MR, Turkenburg JP, Dodson EJ, Martinez-Fleites C, Yang M, Davis BG, Davies GJ, Gilbert HJ. 2007. The crystal structure of two macrolide glycosyltransferases provides a blueprint for host cell antibiotic immunity. Proc Natl Acad Sci U S A 104:5336–5341.

Brown JJ, Zacharin MR. 2009. Safety and efficacy of intravenous zoledronic acid in paediatric osteoporosis. J Pediatr Endocr Metab 22:55–63.

Butters TD, Dwek RA, Platt FM. 2005. Imino sugar inhibitors for treating the lysosomal glycosphingolipidoses. Glycobiology 15:43R–52R.

Costantino-Ceccarini E, Suzuki K. 1975. Evidence for presence of UDP-galactose: ceramide galactosyltransferase in rat myelin. Brain Res 93: 358–362.

Durrant JD, Lindert S, McCammon JA. 2013. AutoGrow 3.0: an improved algorithm for chemically tractable, semiautomated protein inhibitor design. J Mol Graph Model 44:104–112.

Dyer CA, Benjamins JA. 1991. Galactocerebroside and sulfatide independently mediate Ca^{2+} responses in oligodendrocytes. J Neurosci Res 30:699–711.

Hawkins-Salsbury JA, Shea L, Jiang X, Hunter DA, Guzman AM, Reddy AS, Qin EY, Li Y, Gray SJ, Ory DS, Sands MS. 2015. Mechanism-based combination treatment dramatically increases therapeutic efficacy in murine globoid cell leukodystrophy. J Neurosci 35:6495–6505.

Hess B, Kutzner C, van der Spoel D, Lindahl E. 2008. GROMACS 4: algorithms for highly efficient, load-balanced, and scalable molecular simulation. J Chem Theory Comput 4:435–447.

Joshi PG, Mishra S. 1992. Galactocerebroside mediates Ca^{2+} signaling in cultured glioma cells. Brain Res 597:108–113.

Khan AS, Johnston NC, Goldfine H, Schifferli DM. 1996. Porcine 987P glycolipid receptors on intestinal brush borders and their cognate bacterial ligands. Infect Immun 64:3688–3693.

Kopp J, Schwede T. 2004. The Swiss-model repository of annotated three dimensional protein structure homology models. Nucleic Acids Res 32:230–234.

Krieger E, Koraimann G, Vriend G. 2002. Increasing the precision of comparative models with YASARA NOVA: a self-parameterizing force field. Proteins 47:393–402.

Krieger E, Joo K, Lee J, Lee J, Raman S, Thompson J, Tyka M, Baker D, Karplus K. 2009. Improving physical realism, stereochemistry, and side-chain accuracy in homology modeling: four approaches that performed well in CASP8. Proteins 77:114–122.

LeVine SM, Pedchenko TV, Bronshteyn IG, Pinson DM. 2000. L-cycloserine slows the clinical and pathological course in mice with globoid cell leukodystrophy (twitcher mice). J Neurosci Res 60:231–236.

Lezcano V, Bellido T, Plotkin LI, Boland R, Morelli S. 2014. Osteoblastic protein tyrosine phosphatases inhibition and connexin 43 phosphorylation by alendronate. Exp Cell Res 324:30–39.

Li C, Wu Q. 2007. Adaptive evolution of multiple variable exons and structural diversity of drug metabolizing enzymes. BMC Evol Biol 7:69.

Locuson CW, Tracy TS. 2007. Comparative modelling of the human UDP-glucuronyltransferases: insights into structure and mechanism. Xenobiotica 37:155–168.

Mackenzie PI, Bock KW, Burchell B, Guillemette C, Ikushiro SI, Iyanagi T, Miners JO, Owens IS, Nebert DW. 2005. Nomenclature update for the mammalian UDP glycosyltransferase (UGT) gene superfamily. Pharmacogenet Genomics 15:677–685.

Miley MJ, Zielinska AK, Keenan JE, Bratton SM, Radominska-Pandya A, Redinbo MR. 2007. Crystal structure of the cofactor-binding domain of the human phase II drug-metabolism enzyme UDP-glucuronosyltransferase 2B7. J Mol Biol 369:498–511.

Mirsky R, Winter J, Abney ER, Prus RM, Gavrilovic J, Raff MC. 1980. Myelin-specific proteins and glycolipids in rat Schwann cells and oligodendrocytes in culture. J Cell Biol 84:483–494.

Morris GM, Huey R, Lindstrom W, Sanner MF, Belew RK, Goodsell DS, Olson AJ. 1998. Automated docking using a lamarckian genetic algorithm and empirical binding free energy function. J Comput Chem 14:1639–1662.

Offen M, Marinez-Fleites C, Yang M, Lim EK, Davis BG, Tarling CA, Ford CM, Bowles DJ, Davies GJ. 2006. Structure of a flavonoid glucosyltransferase reveals the basis for plant natural product modification. EMBO J 25:1396–1405.

Oostenbrink C, Soares TA, van der Vegt NFA, van Gunsteren WF. 2005. Validation of the 53A6 GROMOS force field. Eur Biophys J 34: 273–284.

Pannuzzo G, Cardile V, Costantino-Ceccarini E, Alvares E, Mazzone D, Perciavalle V. 2010. A galactose-free diet enriched in soy isoflavones and antioxidants results in delayed onset of symptoms of Krabbe disease in twitcher mice. Mol Genet Metab 100:234–240.

Patterson MC, Vecchio D, Prady H, Abel L, Wraith JE. 2007. Miglustat for treatment of Niemann-Pick C disease: a randomised controlled study. Lancet Neurol 6:765–772.

Piotrowska E, Jakóbkiewicz-Banecka J, Tylki-Szymańska A, Liberek A, Maryniak A, Malinowska M, Czartoryska B, Puk E, Kloska A, Liberek T, Barańska S, Węgrzyn A, Węgrzyn G. 2008. The use of genistin-rich isoflavone extract in substrate reduction therapy for Sanfilippo disease: open-label, pilot study in 10 pediatric patients. Curr Ther Res Clin Exp 69:166–179.

Platt FM, Jeyakumar M. 2008. Substrate reduction therapy. Acta Paediatr 97:88–93.

Schäffer AA, Aravind L, Madden TL, Shavirin S, Spouge JL, Wolf YI, Koonin V, Altschul SF. 2001. Improving the accuracy of PSI-BLAST protein database searches with composition-based statistics and other refinements. Nucleic Acids Res 29:2994–3005.

Schulte S, Stoffel W. 1993. Ceramide UDPgalactosyltransferase from myelinating rat brain: purification, cloning, and expression. Proc Natl Acad Sci U S A 90:10265–10269.

Shao H, He X, Achnine L, Blount JW, Dixon RA, Wang X. 2005. Crystal structure of a multifunctional terpene/flavonoid glycosyltransferase from *Medicago trucatula*. Plant Cell 17:3141–3154.

Stahl N, Jurevics H, Morell P, Suzuki K, Popko B. 1994. Isolation, characterization, and expression of cDNA clones that encode rat UDP-galactose: ceramide galactosyltransferase. J Neurosci Res 38:234–242.

Sun HY, Ji FQ, Fu LY, Wang ZY, Zhang HY. 2013. Structural and energetic analyses of SNPs in drug targets and implications for drug therapy. J Chem Inf Model 53:3343-3351.

Takayama S, Chung SJ, Igarashi Y, Ichikawa Y, Sepp A, Lechler RI, Wu J, Hayashi T, Siuzdak G, Wong CH. 1999. Selective inhibition of beta-1,4- and alpha-1,3-galactosyltransferases: donor sugar-nucleotide based approach. Med Chem 7:401–409.

Tanaka K, Webster HD. 1993. Effects of psychosine (galactosylsphingosine) on the survival and the fine structure of cultured Schwann cells. J Neuropathol Exp Neurol 52:490–498.

Trivedi S, Al-Nofal A, Kumar S, Triphati S, Kahoud RJ, Tebben PJ. 2016. Severe noninfective systemic inflammatory response syndrome, shock, and end-organ dysfunction after zoledronic acid administration in a child. Osteoporos Int 27:2379–2382.

Trott O, Olson AJ. 2010. AutoDock Vina: improving the speed and accuracy of docking with a new scoring function, efficient optimization, and multithreading. J Comput Chem 31:455–461.

Vyas VK, Ukawala RD, Ghate M, Chintha C. 2012. Homology modeling a fast tool for drug discovery: current perspectives. Indian J Pharm Sci 74:1–17.

Wong WC, Stroh SM, Eisenhaber F. 2011. Not all transmembrane helices are born equal: towards the extension of the sequence homology concept to membrane proteins. Biol Direct 6:1–30.

Zara S, De Colli M, di Giacomo V, Zizzari VL, Di Nisio C, Di Tore U, Salini V, Gallorini M, Tetè S, Cataldi A. 2015. Zoledronic acid at subtoxic dose extends osteoblastic stage span of primary human osteoblasts. Clin Oral Invest 19:601–611.